Acta Cryst. (1978). B**34**, 64–70

The Crystal Structure of Cu_6PS_5Br, a New Superionic Conductor

BY W. F. KUHS, R. NITSCHE AND K. SCHEUNEMANN

Kristallographisches Institut der Universität Freiburg, Hebelstrasse 25, D-7800 Freiburg im Breisgau, Federal Republic of Germany

(*Received 5 July* 1977; *accepted 8 August* 1977)

Crystals of Cu_6PS_5Br, grown by chemical vapour transport, are cubic, space group $F\bar{4}3m$, $a = 9{\cdot}728$ (1) Å, $Z = 4$. The intensities were measured on an Enraf–Nonius CAD-4 diffractometer. A Patterson synthesis revealed the basic structure. A least-squares refinement, taking into account anisotropic temperature factors, isotropic extinction and anomalous scattering, led to a final R of 0·046. The S and Br anions form a framework of interpenetrating, centred icosahedra (similar to the Laves phase $MgCu_2$), providing ideal and distorted tetrahedral cation sites. The P atoms are coordinated exactly tetrahedrally by four S atoms. The Cu atoms occur in three coordinations: distorted tetrahedral, trigonal planar and linear. The high ionic conductivity is explained by the jumping of Cu atoms between several, only partially occupied, lattice positions.

Introduction

In the course of an investigation of the system Cu–P–S we noted (apart from the known orthothiophosphate Cu_3PS_4) the formation of the new compound Cu_7PS_6 (Kuhs, Schulte-Kellinghaus, Krämer & Nitsche, 1977). Attempts to grow this material by halogen transport resulted in the formation of very stable, cubic copper phosphorus sulphide halides of composition Cu_6PS_5Hal (with Hal = Cl, Br, I). These isomorphic compounds can be synthesized in the pure form from the elements and CuHal at 700 °C. Crystals (orange-red, transparent, flattened tetrahedra, up to 10 × 10 × 4 mm) have been grown by vapour transport (Kuhs, Nitsche & Scheunemann, 1976).

In this paper, the structure of Cu_6PS_5Br is presented and the possible causes for its high ionic conductivity are discussed. Furthermore, the structural relationships to other compounds with icosahedral anion sublattices (in the following termed 'icosahedral structures') are demonstrated [*e.g.* Cd_4GeS_6 (Susa & Steinfink, 1971), Cd_4SiS_6 (Krebs & Mandt, 1972), $Cd_{14}P_4S_{24}$ (Grieshaber, Nitsche & Bubenzer, 1976), $Cd_{13}P_4S_{22}I_2$ (Bubenzer, Nitsche & Grieshaber, 1976), Ag_8GeTe_6 (Rysanek, Laruelle & Katty, 1976), Ag_8SiS_6 (Krebs & Mandt, 1977) and Cu_7PS_6 (Kuhs & Nitsche, 1978)].

Experimental

Crystal data

Vapour-grown, cubic Cu_6PS_5Br crystals show {111} combined with {1$\bar{1}$1} and occasionally {100} and {110} faces. They are orange and transparent (absorption edge at 564 nm). The formula was confirmed by chemical analysis (FW 652·44). Lattice parameters (20 °C) are $a = 9{\cdot}728$ (1) Å, $V = 920{\cdot}6$ (2) Å^3, $Z = 4$, $D_m = 4{\cdot}68$, $D_c = 4{\cdot}707$ Mg m^{-3}. Reflection conditions: hkl: $h + k$, $k + l$, $l + h = 2n$; space group $F\bar{4}3m$. Mo $K\alpha$ radiation ($\lambda = 0{\cdot}7109$ Å), μ(Mo $K\alpha$) = 1·988 m^{-1}. Crystal size: tetrahedron of 180 μm edge length. The cell parameter was obtained by a least-squares refinement of 13 Guinier powder reflections [λ(Cu $K\alpha_1$) = 1·54051 Å; As_2O_3 standard].

Data collection

The crystal was mounted with [100] parallel to the axis of the goniometer. Intensities were collected on a computer-controlled four-circle diffractometer (Enraf–Nonius CAD-4, Mo $K\alpha$ radiation, graphite monochromator) and measured with a scintillation counter. The ω–2θ scan method was used to explore one sixteenth of the sphere of reflection between $2\theta = 7{\cdot}25$ and 116·85°. Long-time drift of the primary beam was corrected by checking the intensities of two standard reflections after every 20 measurements. A total of 634 reflections (255 of which were independent) were recorded. Of these, 171 had intensities $I \geq 2\sigma(I)$, where $\sigma(I)$ is the variance of observations. The internal $R = \Sigma |I - I_m| / \Sigma I_m$ was 0·043 (I_m = mean intensity).

Data reduction

The XRAY 70 system (Stewart, Kundell & Baldwin, 1970) was used for data reduction, structure solution and refinement. Lorentz–polarization and absorption corrections were applied. The absorption corrections (interpolation method of Gauss) varied between 4·87 and 3·22. Scattering factors for Cu, P, S and Br were taken from *International Tables for X-ray Crystallography* (1968).

Structure determination and refinement

Wilson statistics and second-harmonic generation (Nd laser irradiation; $\lambda = 1060$ nm) indicated noncentrosymmetry and uniquely determined the space group as $F\bar{4}3m$.

Peaks in the Patterson map suggested occupancy of: the 24-fold equipoint (*g*), the 16-fold equipoint (*e*) and at least two of the fourfold equipoints (*a*), (*b*), (*c*) or (*d*). The following initial assignments were made: Cu on 24(*g*) with $x = 0$; 16 of the 20 S on 16(*e*) with $x = \frac{3}{8}$; the remaining 4 S on 4(*c*); Br on 4(*a*) and P on 4(*b*). An isotropic structure refinement starting from these positions yielded $R = 0{\cdot}19$.

Fourier and difference maps clearly showed that the Cu atoms were displaced from 24(*g*) into the four different (closely adjoining) equipoints 48(*h*) [Cu(1), Cu(2), Cu(3), Cu(6)], into the equipoint 24(*f*) with $x = \frac{1}{4}$ [Cu(4)] and into 16(*e*) with $x = \frac{1}{8}$ [Cu(5)]. Unrestricted refinement of the Cu atoms yielded population parameters (shown in Table 1) for these equipoints.

Furthermore, the peak heights of the *F* and ΔF maps indicated that the equipoints 4(*a*) and 4(*c*), although fully occupied, must have mixed populations of Br and S atoms. Also, a fraction of the P atoms assigned to 4(*b*) were residing in 4(*d*), both equipoints thus being only partially occupied.

Therefore, a reasonable distribution of four S and four Br on 4(*a*) and 4(*c*) and a partition of four P on 4(*b*) and 4(*d*) had to be established. After finding approximate atomic coordinates by isotropic refinement, *R* was calculated as a function of the distribution of S and Br (all parameters unrestricted, except population parameters of Cu). Mean atomic scattering factors, corresponding to different ratios of S:Br were used, the total number of Br atoms on the two equipoints always being four. A distinct minimum of *R* occurred for 84% Br (16% S) on 4(*a*), symbolized by (Br–S), and 84% S (16% Br) on 4(*c*), symbolized by (S–Br). A subsequent constrained refinement of population parameters for the equipoints 4(*b*) and 4(*d*) indicated that 85% of the four P atoms were residing (in statistical distribution) in 4(*b*) and 15% in 4(*d*). Subsequent unrestricted refinement of the population parameters of the Cu equipoints did not significantly change their values or the position of the minimum in *R*. A least-squares refinement was then carried out with anisotropic temperature factors for all atoms. Isotropic extinction (Larson, 1967) was introduced as an additional parameter and the *f* values were corrected for anomalous scattering. The values of $\Delta f'$ and $\Delta f''$ were taken from *International Tables for X-ray Crystallography* (1974). The function minimized was $\Sigma w(|F_m| - |F_c|)^2$, where $w = 1/\sigma^2(F)$. Refinement was stopped when shifts of all parameters were less than one third of the corresponding standard deviation. The final $R = \Sigma(|F_m| - |F_c|)/\Sigma F_m$ was 0·046.* The ΔF maps now obtained were absolutely flat.

Structural results and discussion

Table 1 gives the atomic coordinates, the percentage occupancy (population parameters) of the various equipoints and the thermal parameters.

The structure is best understood by first considering the anion sublattice formed by S and Br. Sixteen (of the 20) S atoms occupy 16(*e*). The remainder, together with the four Br atoms, are distributed among 4(*a*) and 4(*c*) and denoted (Br–S) and (S–Br) respectively. The

* A list of structure factors has been deposited with the British Library Lending Division as Supplementary Publication No. SUP 32979 (4 pp.). Copies may be obtained through The Executive Secretary, International Union of Crystallography, 13 White Friars, Chester CH1 1NZ, England.

Table 1. *Fractional coordinates, thermal parameters and occupancies*

All values are $\times 10^4$. Estimated standard deviations are in parentheses. The Debye–Waller terms are defined as

$$T = \exp\left(-2\pi^2 \sum_i^3 \sum_j^3 a_i^* a_j^* h_i h_j U^{ij}\right)$$

for Cu(1)–(5) and S, and $T = \exp[-2\pi^2 U^{11}(2\sin\theta/\lambda)^2]$ for Cu(6), P(1), (S–Br) and (Br–S). *W* = Wyckoff position, *P* = % occupancy.

	W	*P*	*x*	*y*	*z*	U^{11}	U^{22}	U^{33}	U^{12}	U^{13}	U^{23}
Cu(1)	48(*h*)	24·5 (8)	2355 (7)	2355 (7)	230 (9)	240 (40)	240 (40)	220 (20)	100 (40)	10 (20)	10 (20)
Cu(2)	48(*h*)	10·5 (2·2)	1940 (20)	1940 (20)	210 (20)	250 (60)	250 (60)	150 (50)	120 (70)	−60 (60)	−60 (60)
Cu(3)	48(*h*)	6·8 (2·1)	1800 (30)	1800 (30)	−130 (40)	440 (120)	440 (120)	390 (190)	−170 (120)	60 (90)	60 (90)
Cu(4)	24(*f*)	8·4 (1·3)	2590 (70)	0	0	880 (290)	630 (150)	630 (150)	0	0	250 (240
Cu(5)	16(*e*)	6·5 (2·1)	1420 (80)	1420 (80)	1420 (80)	930 (370)	930 (370)	930 (370)	490 (420)	490 (420)	490 (420
Cu(6)	48(*h*)	1·8 (7)	2960 (50)	2960 (50)	4810 (60)	170 (90)					
P(1)	4(*b*)	85·0 (5)	5000	5000	5000	70 (10)					
P(2)	4(*d*)	15·0 (5)	7500	7500	7500	710 (340)					
S	16(*e*)	100	6214 (3)	6214 (3)	6214 (3)	146 (7)	146 (7)	146 (7)	−26 (6)	26 (6)	−26 (6)
(S–Br)	4(*c*)	100	2500	2500	2500	210 (10)					
(Br–S)	4(*a*)	100	0	0	0	240 (10)					

anions form a framework of centred, interpenetrating, slightly deformed icosahedra, each anion being surrounded by 12 nearest anion neighbours situated at the vertices of (approximate) icosahedra. In Fig. 1 such a centred anion icosahedron is shown. Its edges, together with the lines connecting the vertices with the centre, form (in the ideal case) 20 trigonal, pseudotetrahedral pyramids. The deformation of each icosahedron is such that two perfect and 18 distorted tetrahedra result (respectively 8 and 128 per unit cell). The two perfect tetrahedra, $T(1)$ and $T(2)$ of Table 2, differing slightly in size, are formed by S atoms only. Among the distorted tetrahedra, which are formed by S, (S–Br) and (Br–S) atoms, four different kinds, $T(3)$–$T(6)$ of Table 2, can be discerned. Thus there exist six kinds of tetrahedral sites in the anion sublattice: two perfect and four deformed. The spatial connexion of the anion icosahedra is conveniently described by a general scheme for coding layered, tetrahedrally close-packed structures (Pearson & Shoemaker, 1969; Shoemaker

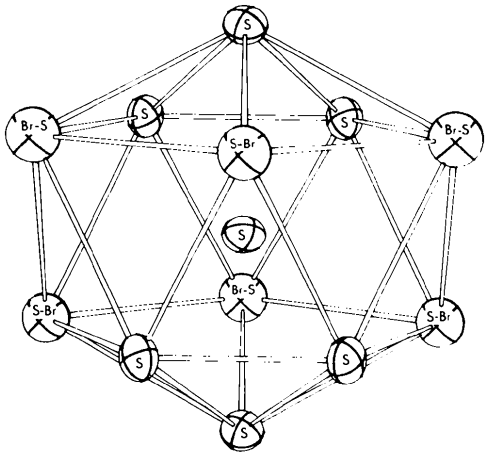

Fig. 1. A centred anion icosahedron with its characteristic pentatomic rings (drawn by *ORTEP*; Johnson, 1965).

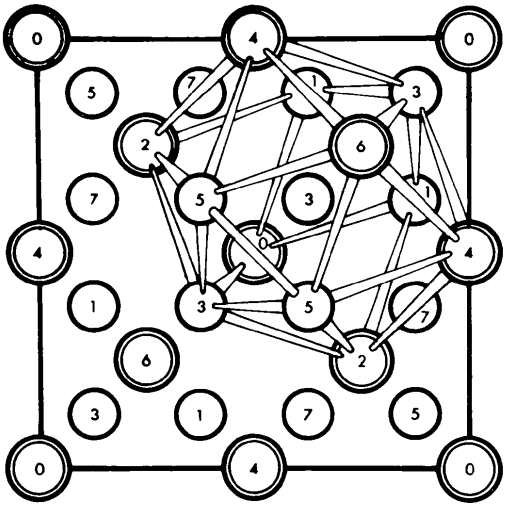

Fig. 2. Projection of the idealized anion sublattice of Cu_6PS_5Br along [100] with an anion icosahedron outlined. The numbers are heights in eighths of the unit cell. Single circles correspond to the Cu atoms, and double circles to the Mg atoms of the Laves phase $MgCu_2$.

Table 2. *Distances and angles in the different anion tetrahedra*

See Table 3 for symmetry code.

	Number per unit cell	Volume (Å^3)	Distances (Å)		Angles (°)		Examples
$T(1)$	4	4·39	S–S	3·340 (4)	S–S–S	60·00 (9)	S, S^{iv}, S^{vi}, S^{vii}
$T(2)$	4	5·22	S–S	3·538 (4)	S–S–S	60·00 (8)	S, S^{viii}, S^{iv}, S^{v}
$T(3)$	16	5·69	(S–Br)–S	4·023 (3)	(S–Br)–S–S	65·47 (7)	(S–Br), S^{ii}, S^{iii}, S^{vi}
			S–S	3·340 (4)	S–(S–Br)–S	49·06 (6)	
					S–S–S	60·00 (9)	
$T(4)$	16	6·31	(Br–S)–S	4·044 (3)	(Br–S)–S–S	63·91 (7)	(Br–S), S^{iii}, S^{iv}, S^{xii}
			S–S	3·538 (4)	S–(Br–S)–S	51·89 (6)	
					S–S–S	60·00 (8)	
$T(5)$	48	7·33	(Br–S)–(S–Br)	4·212	(Br–S)–(S–Br)–S	58·77 (4)	(Br–S), (S–Br), S^{i}, S^{ii}
			(Br–S)–S	4·044 (3)	(S–Br)–(Br–S)–S	58·28 (4)	
			(S–Br)–S	4·023 (3)	(Br–S)–S–(S–Br)	62·96 (4)	
			S–S	3·340 (4)	(Br–S)–S–S	65·61 (6)	
					(S–Br)–S–S	65·47 (6)	
					S–(Br–S)–S	51·89 (6)	
					S–(S–Br)–S	52·18 (6)	
$T(6)$	48	7·05	(Br–S)–(S–Br)	4·212	(Br–S)–(S–Br)–S	58·77 (4)	(Br–S), (S–Br), S^{ii}, S^{iii}
			(Br–S)–S	4·044 (3)	(S–Br)–(Br–S)–S	58·28 (4)	
			(S–Br)–S	4·023 (3)	(Br–S)–S–(S–Br)	62·96 (4)	
			S–S	3·538 (4)	(Br–S)–S–S	64·06 (6)	
					(S–Br)–S–S	63·91 (6)	
					S–(Br–S)–S	48·79 (6)	
					S–(S–Br)–S	49·06 (6)	

& Shoemaker, 1972). In this scheme, the (simplified) code for the icosahedral anion sublattice is $P(0; L)$ (Bubenzer, Nitsche & Grieshaber, 1976). It is interesting to note that the same code also applies to the Laves phase $MgCu_2$. In fact, as shown in Fig. 2, the idealized anion sublattice of Cu_6PS_5Br (and of many other icosahedral structures) is identical with the $MgCu_2$ lattice. The 16 S atoms in 16(*e*) correspond to the Cu atoms, and the 'atoms' (S–Br) and (Br–S) in 4(*c*) and 4(*a*) respectively correspond to the Mg atoms in $MgCu_2$.

Optimal packing in such an icosahedral arrangement requires two constituents in the proportion $A:B = 1:2$ having a radius ratio of $r_A:r_B = \sqrt{3}:\sqrt{2} = 1{\cdot}225$. For $MgCu_2$ this ratio is 1·250. For Cu_6PS_5Br it is only 1·065 and in addition there is a deficiency in the larger constituent (Br) which has to be compensated by filling the gaps in its sites by atoms of the smaller constituent (S). This causes high temperature factors for the (S–Br) and (Br–S) 'atoms' in the structure.

All equipoints of the cation sublattice, on the other hand, are only partially occupied.

The P atoms reside in the smallest (the perfect) tetrahedral sites of the anion sublattice: P(1) in $T(1)$ with 85% occupancy and P(2) in $T(2)$ with 15% occupancy (see Table 2). The 24 Cu atoms are distributed among six partially (and statistically) occupied equipoints which correspond to various locations within the distorted anion tetrahedra. A total of 87% of the Cu atoms [Cu(1), Cu(2), Cu(3) and Cu(6)] reside in four different 48-fold equipoints with widely differing occupancies. The remaining 13% [Cu(4), Cu(5)] reside in 24(*f*) and 16(*e*). The total number of Cu atoms on independently refined positions is 24·0 ± 1·6 per cell, confirming the chemical analysis.

Cu(1) is situated close to the centre of one face of the (distorted) anion tetrahedron $T(6)$. Its coordination is, therefore, nearly triangular. Cu(2) and Cu(3) are situated near the centre of $T(6)$ and thus are coordinated approximately tetrahedrally. Table 3 gives the bond lengths and angles of the Cu and P environments. Fig. 3 shows the environments, typical distances and thermal ellipsoids of Cu(1) – Cu(3). Cu(4), lying on a face of $T(5)$, is also coordinated triangularly. Cu(5) is situated on an (S–Br)–(Br–S) edge of $T(6)$ and, therefore, is exactly linearly coordinated by two anions. Cu(6) is nearly linearly coordinated by two S atoms. The short Cu(6)–S distance of 1·77 Å is notable. The reason for the presence of Cu atoms in the weakly populated position Cu(6) is probably the partial occupancy of the P equipoints 4(*b*), 15% of which are empty. Therefore, a fraction of the Cu(1) – Cu(3) atoms shift into position Cu(6) towards the empty P equipoints 4(*b*).

At this point it should be mentioned that Cu_6PS_5Br exhibits a high conductivity caused by migration of Cu ions. At 30 °C the ionic conductivity is $1{\cdot}5 \times 10^{-7}\ \Omega^{-1}\ m^{-1}$, at 250 °C it reaches $3{\cdot}4 \times 10^{5}\ \Omega^{-1}\ m^{-1}$. Its thermal activation energy is 0·35 eV. An insight into the possible conductivity mechanisms can be obtained by considering the positions of the Cu atoms and the directions of their thermal ellipsoids.

Cu(1) – Cu(3) are located within (distorted) tetrahedra of the type $T(6)$ (see Fig. 3). The relative close vicinity of these positions makes it appear probable that jumps of Cu ions between them are easily thermally activated. An explanation of the migration of Cu ions into adjacent anion tetrahedra is offered by the fact that the longest axes of the (highly anisotropic) thermal ellipsoids of Cu(2) and Cu(3) are directed towards

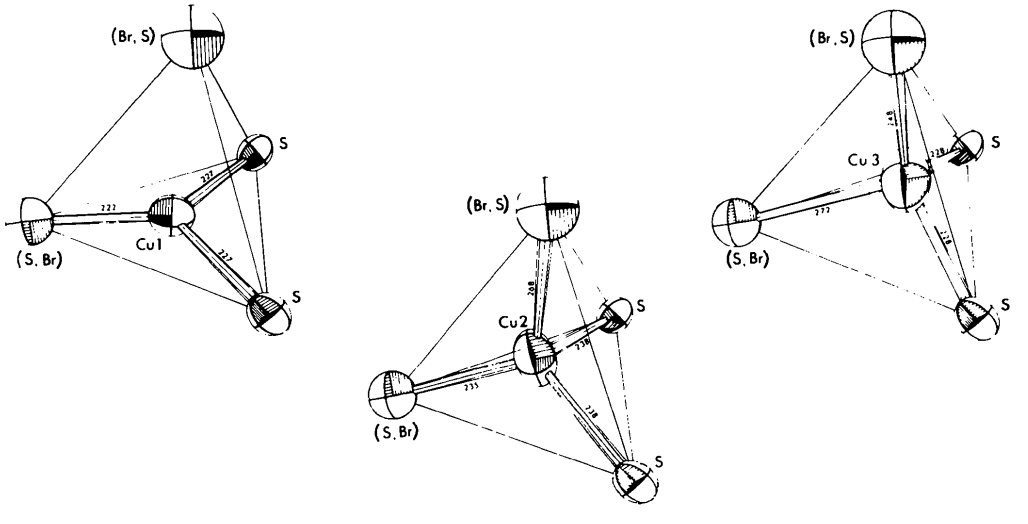

Fig. 3. Environments and anisotropic thermal ellipsoids of Cu(1) – Cu(3) (drawn by *ORTEP*: Johnson, 1965). (Note: distances are in pm.)

Cu(5) and Cu(4) respectively. The latter atoms lie on (S–Br)–(Br–S) edges and on S–S–(Br–S) faces, respectively, of $T(5)$, $T(6)$ tetrahedra. The positions Cu(2) and Cu(3) can thus be considered as starting points for thermally activated jumps of Cu ions into the positions Cu(5) and Cu(4) respectively, from where, by analogous processes, they can reach Cu(2) or Cu(3) positions in neighbouring tetrahedra *etc.* Fig. 4 is a perspective drawing of $T(5)$ and $T(6)$ anion tetrahedra from a section of the lattice, showing these two plausible jumping processes for the Cu ions. The Cu(2)–Cu(5)–Cu(2) process (jump distance 1·37 Å) takes place *via* the common edge of two $T(6)$ tetrahedra (see Table 2). In the Cu(3)–Cu(4)–Cu(3) process (jump distance 1·90 Å) a Cu(3) from $T(6)$ traverses one $T(5)$, reaches the position Cu(4) on the common face of two $T(5)$ tetrahedra, traverses the second $T(5)$ and finally lands in position Cu(3) of another $T(6)$. The plausibility of these processes is further substantiated by the fact that Cu(4) and Cu(5) have very high anisotropic temperature factors and low site occupancies, indicating a short duration of stay of Cu ions on these sites during their migration. The low temperature factor of Cu(6) indicates that atoms on equipoints 48(*h*), which are weakly populated anyway, do not participate appreciably in the jumping process.

Fig. 5 is an electron density map of the cell at $x = 0$, indicating the pathways of the process Cu(3)–Cu(4)–Cu(3).

The partial occupancy of the P equipoints 4(*b*) and 4(*d*) is also of consequence to ionic conduction. Suppose all four P atoms (fully) occupy 4(*b*) as P(1) (see Fig. 5). Then, because of the high positive charge of P^{5+}, the Cu(4) sites, important stations for the Cu(3)–Cu(4)–Cu(3) jumping process, would not be occupied [distance P(1)–Cu(4) 2·35 Å]. Jumping of Cu(3) from one tetrahedron to another *via* position

Table 3. *Bond lengths* (Å) *and angles* (°) *of the* Cu *and* P *environments*

Standard deviations are in parentheses.

Cu(1)–(S–Br)	2·218 (9)	(S–Br)–Cu(1)–S^{i}	127·5 (4)
Cu(1)–S^{i}	2·268 (8)	(S–Br)–Cu(1)–S^{ii}	127·5 (4)
Cu(1)–S^{ii}	2·268 (8)	(S–Br)–Cu(1)–(Br–S)	99·1 (3)
Cu(1)–(Br–S)	3·248 (7)	S^{i}–Cu(1)–S^{ii}	102·6 (4)
		S^{i}–Cu(1)–(Br–S)	92·6 (2)
		S^{ii}–Cu(1)–(Br–S)	92·6 (2)
Cu(2)–(S–Br)	2·35 (2)	(S–Br)–Cu(2)–S^{i}	116·5 (8)
Cu(2)–S^{i}	2·38 (2)	(S–Br)–Cu(2)–S^{ii}	116·5 (8)
Cu(2)–S^{ii}	2·38 (2)	(S–Br)–Cu(2)–(Br–S)	113·6 (8)
Cu(2)–(Br–S)	2·68 (2)	S^{i}–Cu(2)–S^{ii}	96·2 (7)
		S^{i}–Cu(2)–(Br–S)	106·2 (7)
		S^{ii}–Cu(2)–(Br–S)	106·2 (7)
Cu(3)–S^{i}	2·27 (3)	S^{i}–Cu(3)–S^{ii}	102 (1)
Cu(3)–S^{ii}	2·27 (3)	S^{i}–Cu(3)–(Br–S)	117 (1)
Cu(3)–(Br–S)	2·48 (3)	S^{i}–Cu(3)–(S–Br)	106 (1)
Cu(3)–(S–Br)	2·74 (4)	S^{ii}–Cu(3)–(Br–S)	117 (1)
		S^{ii}–Cu(3)–(S–Br)	106 (1)
		(Br–S)–Cu(3)–(S–Br)	108 (1)
Cu(4)–S^{ii}	2·04 (4)	S^{ii}–Cu(4)–S^{iii}	110 (3)
Cu(4)–S^{iii}	2·04 (4)	S^{ii}–Cu(4)–(Br–S)	125 (2)
Cu(4)–(Br–S)	2·52 (7)	S^{iii}–Cu(4)–(Br–S)	125 (2)
Cu(5)–(S–Br)	1·83 (8)	(S–Br)–Cu(5)–(Br–S)	180
Cu(5)–(Br–S)	2·38 (8)		
Cu(6)–S^{iv}	1·77 (6)	S^{iv}–Cu(6)–(S–Br)	156 (3)
Cu(6)–(S–Br)	2·34 (6)	S^{iv}–Cu(6)–S^{v}	100 (3)
Cu(6)–S^{v}	2·77 (5)	(S–Br)–Cu(6)–S^{v}	104 (2)
P(1)–S	2·045 (3)	S–P(1)–S^{vi}	109·5 (1)
P(1)–S^{vi}	2·045 (3)	S–P(1)–S^{vii}	109·5 (1)
P(1)–S^{vii}	2·045 (3)	S–P(1)–S^{iv}	109·5 (1)
P(1)–S^{iv}	2·045 (3)	S^{vi}–P(1)–S^{vii}	109·5 (1)
		S^{vi}–P(1)–S^{iv}	109·5 (1)
		S^{vii}–P(1)–S^{iv}	109·5 (1)
P(2)–S	2·167 (3)	S–P(2)–S^{v}	109·5 (1)
P(2)–S^{v}	2·167 (3)	S–P(2)–S^{viii}	109·5 (1)
P(2)–S^{viii}	2·167 (3)	S–P(2)–S^{iv}	109·5 (1)
P(2)–S^{iv}	2·167 (3)	S^{v}–P(2)–S^{viii}	109·5 (1)
		S^{v}–P(2)–S^{iv}	109·5 (1)
		S^{viii}–P(2)–S^{iv}	109·5 (1)

Superscripts refer to the following transformations

None	x, y, z	(viii)	$-x+\frac{3}{2}, -y+\frac{3}{2}, z$
(i)	$x-\frac{1}{2}, -y+1, -z+\frac{1}{2}$	(ix)	$-x+\frac{3}{2}, y, -z+\frac{3}{2}$
(ii)	$-x+1, y-\frac{1}{2}, z+\frac{1}{2}$	(x)	$x, -y+\frac{3}{2}, -z+\frac{1}{2}$
(iii)	$-x+1, -y+\frac{1}{2}, z-\frac{1}{2}$	(xi)	$x, y-\frac{1}{2}, z-\frac{1}{2}$
(iv)	$-x+1, -y+1, z$	(xii)	$x-1, y-\frac{1}{2}, z-\frac{1}{2}$
(v)	$x-\frac{1}{2}, y-\frac{1}{2}, z$	(xiii)	$-x+\frac{1}{2}, y-\frac{1}{2}, -z+1$
(vi)	$x, -y+1, -z+1$	(xiv)	$-x+\frac{1}{2}, -y+1, z-\frac{1}{2}$
(vii)	$-x+1, y, -z+1$		

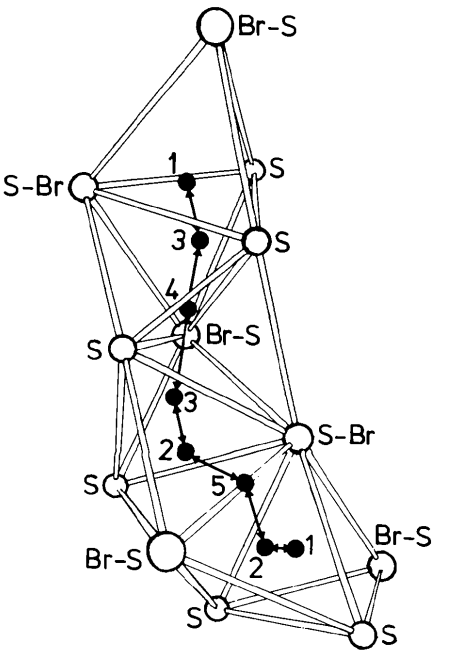

Fig. 4. Pathways of Cu ions for the jumping processes Cu(3)–Cu(4)–Cu(3) and Cu(2)–Cu(5)–Cu(2) in a section of the lattice. The sequence shown has been arbitrarily chosen from many possible ones (drawn by *ORTEP*: Johnson, 1965).

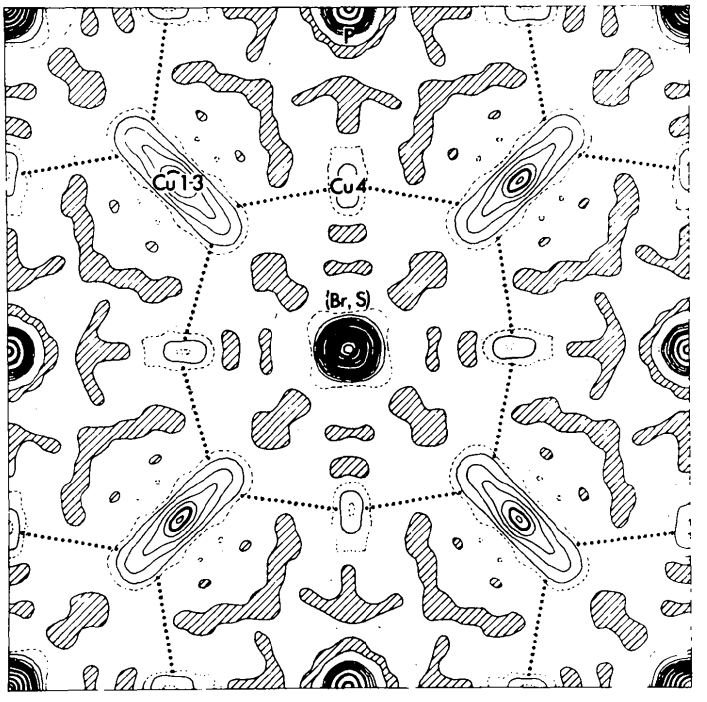

Fig. 5. Electron density map of the unit cell at $x = 0$ (not scaled). Heavily dotted lines indicate probable pathways of Cu$^+$ ions for Cu(3)–Cu(4)–Cu(3) processes. Hatched areas have negative densities of less than 1 e Å^{-2}.

Cu(4), therefore, is only probable if the P positions adjoining Cu(4) are not occupied.

The high temperature factors of (Br–S) and (S–Br), mentioned above, make it highly probable that the Cu jumping processes are, in addition, facilitated by coupled oscillations of these atoms. Their disordered distribution makes the lattice 'softer' than for icosahedral packing containing the two constituents (as in $MgCu_2$) in the proper quantities (1:2) and radius ratios.

Icosahedral anion sublattices appear to exist in many chalcogenides and chalcogenide halides. The first representatives found were the isomorphic compounds Cd_4GeS_6 (Susa & Steinfink, 1971) and Cd_4SiS_6 (Krebs & Mandt, 1972) which are monoclinic, space group *Cc*, $Z = 4$. The S tetrahedra containing the small atoms Si or Ge (corresponding to P in Cu_6PS_5Br) are highly regular, while those containing Cd (corresponding to Cu in Cu_6PS_5Br) are quite distorted. Low-temperature X-ray photographs (Kuhs, Nitsche & Scheunemann, 1976) indicate that Cu_6PS_5Br transforms at about −95 °C into a monoclinic modification which, because of the similarity of the powder patterns, seems to be isotypic with Cd_4SiS_6 and Cd_4GeS_6. The P analogue of the latter two compounds has also been prepared. Its unit-cell content is $Cd_{14}P_4S_{24}$ (Grieshaber, Nitsche & Bubenzer, 1976) and it is also monoclinic, *Cc*, at room temperature. This compound constitutes an end member of the mixed-crystal series $Cd_{14-x}P_4S_{24-2x}I_{2x}$ with $0 \le x \le 1$. The other end member is $Cd_{13}P_4S_{22}I_2$. By a special growth technique, the cubic ($F\bar{4}3m$) high-temperature phase of the latter compound can be stabilized at room temperature. It is interesting to compare its structure (Bubenzer, Nitsche & Grieshaber, 1976) with that of Cu_6PS_5Br. Whereas the anion sublattices are very similar, the most important difference is that in $Cd_{13}P_4S_{22}I_2$ all four P atoms occupy one equipoint [4(*b*)]. In Cu_6PS_5Br they partially populate two equipoints [4(*b*) and 4(*d*)] in a statistical manner. In $Cd_{13}P_4S_{22}I_2$ the Cd atoms are distributed among the distorted anion tetrahedra in such a way that only corner-sharing, Cd-containing tetrahedra result. (The Cd–Cd distances between atoms residing in edge-sharing tetrahedra would be shorter than the interatomic distance in Cd metal of 2·98 Å.) In Cu_6PS_5Br, on the other hand, the Cu atoms are distributed such that edge-sharing, occupied tetrahedra also occur. The distance between adjacent Cu(3) atoms in edge-sharing anion tetrahedra is 2·65 Å, which is longer than the shortest Cu–Cu distances in comparable compounds (Cu_2S 2·53 Å, $CuBi_5S_8$ and Cu metal 2·56 Å; Ohmasa & Mariolacos, 1974). Simultaneous occupation of face-sharing anion tetrahedra is impossible in both $Cd_{13}P_4S_{22}I_2$ and Cu_6PS_5Br, where the Cu(3)–Cu(3) distance would be 1·93 Å.

Other icosahedral compounds described recently are: Ag_8SiS_6 ($Pna2_1$, $Z = 4$; Krebs & Mandt, 1977), Ag_8GeTe_6 ($F\bar{4}3m$, $Z = 4$; Rysanek, Laruelle & Katty, 1976) and Ag_9GaS_6 (orthorhombic *I* lattice, $Z = 4$;

Brandt & Krämer, 1976). We shall soon report on new compounds of the types $A_7M^{IV}Ch_5Hal$ and $A_6M^{V}Ch_5Hal$ (A = Cu, Ag; M^{IV} = Si, Ge; M^{V} = P, As; Ch = S, Se, Te; Hal = Cl, Br, I) with $Z = 4$ and on the mixed-crystal series $Cu_{6-3x}In_{6+x}P_4S_{20}Hal_4$ with $Z = 1$. In all these materials the (small) Ga, Si, Ge, P or As atoms, preferring highly regular coordination, are located in the ideal tetrahedra of the icosahedral anion sublattice consisting of S, Se or Te, partly with Cl, Br or I. The atoms Cu, Ag, Cd (Hg), which may occur in various (less regular) coordinations, are located in the distorted tetrahedra or are coordinated by only three (two) anions in a triangular (linear) fashion. Icosahedral compounds can crystallize in various typical lattices, between which phase transitions occur, and which derive (by various ordering processes) from a common high-temperature phase of space group $F\bar{4}3m$.

In ternary sulphides, selenides and tellurides, icosahedral anion coordination seems to be favoured over cubo-octahedral anion coordination (as in cubic close packing and hexagonal close packing) if (1) one of the two cations present (*e.g.* Si^{4+}, Ge^{4+}, P^{5+}, As^{5+}) has a strong preference for exact tetrahedral coordination, whereas the other (*e.g.* Cu^{+}, Ag^{+}, Cd^{2+}, Hg^{2+}) settles for less symmetric (distorted tetrahedral, trigonal-planar or linear) coordination (2) the chalcogenide sublattice is partially substituted by halogen. The resulting mixed-anion sublattice, although, as discussed above for $MgCu_2$, far from fulfilling the geometric conditions for ideal icosahedral packing, nevertheless favours its formation.

Icosahedral compounds thus constitute a widespread class of materials, allowing a large variety of chemical substitution and corresponding changes in physical properties. Their noncentrosymmetric structures make them attractive candidates for studying piezoelectric, pyroelectric and electro-optic effects (Grieshaber, Nitsche & Bubenzer, 1976). Those containing Cu and Ag anions are potential superionic conductors.

The authors thank Dr W. Littke for the intensity measurements and Dr U. van Alpen for an introduction to ionic-conductivity measurements during two periods at Max-Planck-Institut für Festkörperforschung in Stuttgart, Federal Republic of Germany.

All calculations were carried out on the Univac 1106-II computer of the Rechenzentrum der Universität Freiburg. Financial support from the Deutsche Forschungsgemeinschaft is gratefully acknowledged.

References

Brandt, G. & Krämer, V. (1976). *Mater. Res. Bull.* **11**, 1381–1388.

Bubenzer, A., Nitsche, R. & Grieshaber, E. (1976). *Acta Cryst.* B**32**, 2825–2829.

Grieshaber, E., Nitsche, R. & Bubenzer, A. (1976). *Mater. Res. Bull.* **11**, 1169–1177.

International Tables for X-ray Crystallography (1968). Vol. III, 2nd ed. Birmingham: Kynoch Press.

International Tables for X-ray Crystallography (1974). Vol. IV. Birmingham: Kynoch Press.

Johnson, C. K. (1965). *ORTEP*. Report ORNL-3794, revised. Oak Ridge National Laboratory, Tennessee.

Krebs, B. & Mandt, J. (1972). *Z. Anorg. Allg. Chem.* **338**, 193–206.

Krebs, B. & Mandt, J. (1977). *Z. Naturforsch. Teil B*, **32**, 24–30.

Kuhs, W. F. & Nitsche, R. (1978). *Acta Cryst.* To be published.

Kuhs, W. F., Nitsche, R. & Scheunemann, K. (1976). *Mater. Res. Bull.* **11**, 1115–1124.

Kuhs, W. F., Schulte-Kellinghaus, M., Krämer, V. & Nitsche, R. (1977). *Z. Naturforsch. Teil B*, **32**, 1100–1101.

Larson, A. C. (1967). *Acta Cryst.* A**26**, 71–83.

Ohmasa, M. & Mariolacos, K. (1974). *Acta Cryst.* B**30**, 2640–2643.

Pearson, W. B. & Shoemaker, C. B. (1969). *Acta Cryst.* B**25**, 1178–1183.

Rysanek, N., Laruelle, P. & Katty, A. (1976). *Acta Cryst.* B**32**, 692–696.

Shoemaker, C. B. & Shoemaker, D. P. (1972). *Acta Cryst.* B**28**, 2957–2965.

Stewart, J. M., Kundell, F. A. & Baldwin, J. C. (1970). The XRAY 70 system. Computer Science Center, Univ. of Maryland, College Park, Maryland.

Susa, K. & Steinfink, H. (1971). *Inorg. Chem.* **10**, 1754–1756.